
Light Localization by Defects in Optically Induced Photonic Structures

Jianke Yang¹, Xiaosheng Wang², Jiandong Wang¹, and Zhigang Chen^{2,3}

¹ Department of Mathematics and Statistics, University of Vermont, VT 05401, USA

jyang@cems.uvm.edu, jwang@cems.uvm.edu

² Department of Physics and Astronomy, San Francisco State University, CA 94132, USA

gxkren@gmail.com, zchen@stars.sfsu.edu

³ TEDA Applied Physical School, Nankai University, Tianjin 300457, China

7.1 Introduction

In the past ten years, there has blossomed an interest in the study of collective behavior of wave propagation in periodic waveguide arrays and photonic lattices [1–3]. The unique bandgap structures of these periodic media, coupled with nonlinear effects, give rise to many types of novel soliton structures [1–26]. On the other hand, it is well known that one of the unique and most interesting features of photonic band-gap structures is a fundamentally different way of waveguiding by defects in otherwise uniformly periodic structures. Such waveguiding has been demonstrated with an “air-hole” in photonic crystal fibers (PCF) for optical waves [27, 28], in an isolated defect in two-dimensional arrays of dielectric cylinders for microwaves [29–31], and recently in all-solid PCF with a lower-index core [32, 33]. In addition, laser emission based on photonic defect modes has been realized in a number of experiments [34–38]. In one-dimensional (1D) fabricated semiconductor waveguide arrays, previous experiments have investigated nonlinearity-induced escape from a defect state [39] and interactions of discrete solitons with structural defects [40] (see also [41]).

Despite the above efforts, theoretical understanding on defect guiding was still limited, and experimental demonstrations of defect guiding was still scarce. In addition, when nonlinear effects are significant, how defect guiding is affected by nonlinearity is largely an open issue. Recently, in a series of theoretical and experimental studies, we optically induced 1D, 2D and ring-like photonic lattices with single-site negative defects in photorefractive crystals, and investigated their linear and nonlinear light guiding properties [42–48]. This work will be reviewed in this Chapter. In addition, we present the first experimental demonstration of nonlinear defect modes which undergoes nonlinear

propagation through the defects. Our work not only has a direct link to technologically important systems of periodic structures such as PCF, but also brings about the possibility for studying, in an optical setting, many novel phenomena in periodic systems beyond optics such as edge dislocation, defect healing, eigenmode splitting, and nonlinear mode coupling which have been intriguing scientists for decades [49–51].

7.2 Optically Induced Lattices and Defects

With today's nano-fabrication technology, creation of a closely-spaced uniform 1D waveguide array on a substrate material is not a difficult task. For instance, such waveguides have been fabricated with AlGaAs semiconductor materials or LiNbO₃ crystals. Yet, it has been a challenge to create or fabricate 2D or 3D waveguide arrays in bulk media. In Ref. [9], 2D photonic lattices were successfully created by sending multiple interfering beams into a crystal. This interference method has some disadvantages, such as its sensitivity to ambient perturbation, and its inability to generate more complicated lattice structures with single-site defects. In view of that, we used a different method of optical induction which is based on the amplitude modulation of a partially coherent optical beam.

The experimental setup for our study is illustrated in Fig. 7.1. The experiments are performed in a biased SBN:60 (strontium barium niobate) photorefractive crystal (typically, $r_{33} \sim 280$ pm/V and $r_{13} \sim 24$ pm/V) illuminated by a laser beam (either Coherent argon ion laser $\lambda = 488$ nm or solid-state laser $\lambda = 532$ nm) passing through a rotating diffuser and an amplitude mask. The biased crystal (bias field can be varied from -2.0 to 6.0 kV/cm) provides

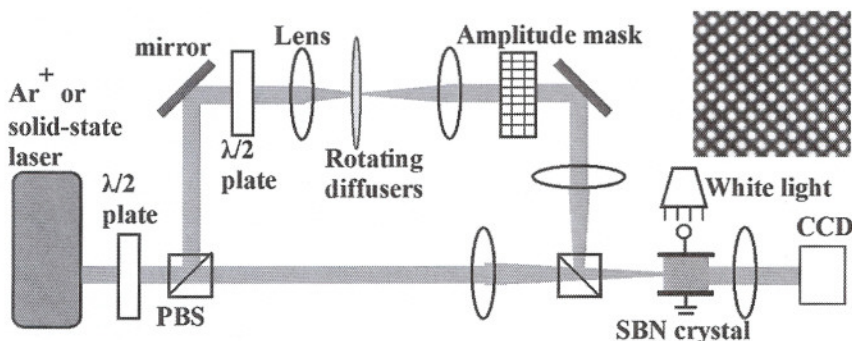


Fig. 7.1. Experimental setup for optical induction of waveguide lattices in a biased photorefractive crystal by amplitude modulation of a partially coherent beam. PBS: polarizing beam splitter, SBN: strontium barium niobate. Top path is the lattice beam, and bottom path is the probe beam (either a Gaussian beam or a vortex beam if a vortex mask is inserted). The right insert shows a typical experimental picture of 2D uniform lattice created by optical induction

a self-focusing or defocusing noninstantaneous nonlinearity [52]. The rotating diffuser turns the laser beam into a partially spatially incoherent beam with controllable degree of spatial coherence, as first introduced in experiments with incoherent optical solitons [53–55]. The amplitude mask provides spatial modulation after the diffuser on the otherwise uniform beam, which exhibits a periodic intensity pattern at the input face of the crystal [56,57]. This partially coherent and spatially modulated beam is used as our lattice beam. Another beam, either split from the same laser or emitted from a different laser and not passing through the diffuser and the mask, is used as our probe beam, propagating along with the lattice. In our experiments on defect modes, the lattice beam has its polarization close to being o-polarized, thus the lattice beam induces a weak periodic index variation to form the waveguide arrays. The probe beam, on the other hand, is always a coherent e-polarized beam, but its intensity and/or wavelength can be adjusted so it can undergo linear propagation (for study of linear guidance or linear defect modes) or nonlinear propagation (for study of nonlinear trapping or nonlinear defect modes) as detailed in later sections. The two beams are monitored separately with CCD cameras at the input and output facets of the crystal. In addition, a white-light background beam illuminating from the top of the crystal is normally used for fine-tuning the photorefractive nonlinearity [52–60].

In our experiments, the periodic lattice must stay stationary during its quasi-linear propagation through the crystal. In order for this to happen, we need to understand how to eliminate the *Talbot effect*. The Talbot effect is a phenomenon of coherent light propagation in a homogeneous media with spatially-periodic initial conditions [61,62]. Light exhibiting this phenomenon does not propagate stationarily, and it shrinks and expands as it moves along, and its intensity pattern repeats itself periodically along the propagation direction. Our lattice beam travels in a homogeneous crystal (as it does not feel the probe beam), and its initial condition on the input face of the crystal is periodic (due to the amplitude mask). Because of the Talbot effect, it can not form a stationary lattice. To overcome this difficulty, our idea is to use frequency filtering to remove half of the spatial frequencies in the initial conditions. The filtered lattice beam, when slightly tilted, can propagate stationarily along the crystal; thus, the Talbot effect is eliminated. Our experimentally created 1D and 2D stationary lattices are presented in Fig. 7.2. A theoretical understanding for the elimination of the Talbot effect by frequency filtering and beam tilting can be found in [63].

In our studies, we need to optically create stationary periodic lattices with a local defect akin to an “air defect” in photonic crystals. To explore this possibility, we prepare an initial periodic lattice with a single-site negative defect using amplitude masks. Under linear propagation, however, we find that the frequency filtering and beam tilting techniques are not enough to maintain the defect and keep the lattice stationary. The defect tends to be washed out at the exit face of the crystal. In order to maintain the defect, we employ two additional techniques. One is to introduce a small amount of nonlinearity

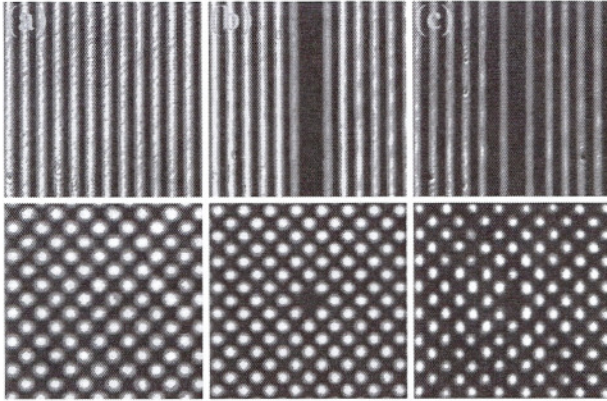


Fig. 7.2. Optically induced 1D and 2D lattices with a single-site negative defect, as obtained from our experiments. 1D results (*top*), 2D results (*bottom*). (a) uniform lattice at output, lattice spacing $42\ \mu\text{m}$ (1D) and $27\ \mu\text{m}$ (2D), (b) lattice with defect at input, (c) lattice with defect at output maintained by weak nonlinearity

into the lattice beam (by setting its polarization to contain a small amount of e-polarized component), and the other one is to introduce partial incoherence into the lattice beam (by letting the lattice beam go through a rotating diffuser). With the combined use of these techniques, we have successfully created 1D and 2D single-site defects in the otherwise uniform lattice which remains nearly stationary throughout the crystal (length varies from 10 to 20 mm). Typical examples are presented in Fig. 7.2.

7.3 Linear Defect Modes in 1D Lattices

When a periodic lattice has a local defect, this defect can affect the propagation of a probe beam significantly and in a way fundamentally different from linear propagation in continuous media. For instance, if the defect is negative (repulsive), i.e., the lattice intensity at the defect is lower than that in neighboring lattice sites, the defect can guide a linear localized mode (defect mode). This is quite counter-intuitive. The physical mechanism for this unusual light guiding is the repeated Bragg reflections, rather than the conventional total internal reflections, analogous to light transmission in air-hole photonic crystal fibers.

To understand the linear light-guiding property of a negative defect, a theoretical analysis is performed first for our present physical system [42, 43]. The non-dimensionalized model is [7–9]

$$iU_z + U_{xx} - \frac{E_0}{1 + I_L(x)}U = 0, \quad (7.1)$$

where U is the envelope function of the probe beam, E_0 is the applied bias field, $I_L(x) = I_0 \cos^2(x)[1 - f_D(x)]$ is the lattice intensity containing a defect, I_0 is the lattice peak intensity, and $f_D(x) = \exp(-x^8/128)$ accounts for the single-site negative defect. If we take $I_0 = 3$, this defective lattice is shown in Fig. 7.3i. A surprising fact is that this negative defect supports localized defect modes (DMs) of the form

$$U(x, z) = u(x)e^{-i\mu z}, \quad (7.2)$$

where μ is the propagation constant (DM eigenvalue). These eigenvalues versus E_0 are shown in Fig. 7.3ii. It is seen that these eigenvalues all lie in the gaps between Bloch bands. None of them exists in the semi-infinite bandgap (total internal reflection region). As E_0 increases, these modes disappear from lower bandgaps, and appear in higher bandgaps. A typical DM profile in the second gap is shown in Fig. 7.3iii. This mode has its intensity maximum inside the negative defect, with double-peaks in each lattice spacing, and its neighboring intensity peaks are out of phase with each other [42, 43].

The above results on DMs are confirmed experimentally, and our experimental results are shown in Fig. 7.3a–d. Here, Fig. 7.3a is the input of the 1D lattice with a defect (lattice spacing about $42\mu\text{m}$), the polarization angle

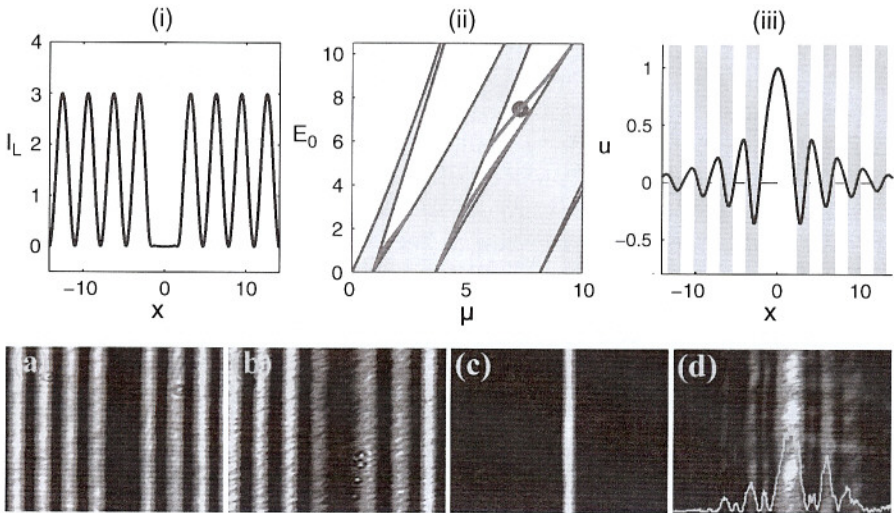


Fig. 7.3. Theoretical demonstration of defect modes (*top*). (i) Lattice intensity profile, (ii) DM branches in the (μ, E_0) plane, (iii) a DM in the second bandgap marked by a circle in (ii). Experimental observation of DMs (*bottom*), shown are transverse intensity patterns of the lattice beam at crystal input (a) and output (b) with a single-site defect, and those of the probe beam at input (c) and output (b) after 20 mm propagation through the defect channel. Lattice spacing $42\mu\text{m}$, Bias field 1.1 kV/cm (after Ref. [42, 43, 46])

is about 8% relative to the o-axis, and the propagation distance is 20 mm. At the bias field of 1.1 kV/cm, the output of the lattice is shown in Fig. 7.3b. It is seen that the defect is well maintained throughout propagation. After such a lattice is “fabricated”, its light guiding property can be studied. To do so, we launch a low-intensity e-polarized probe beam into the defect. The experimental result is shown in Figs. 7.3c and 7.3d. It can be seen that after 20 mm propagation, most of the probe-beam energy is still confined inside the negative defect. This is remarkable, as without the defect, the probe beam would strongly scatter to nearby lattice sites in case of strong coupling. The experimentally observed defect mode (Fig. 7.3d) closely resembles the theoretical one in Fig. 7.3iii.

7.4 Linear Defect Modes in 2D Square Lattices

Guiding light by defects in 2D periodic lattices is even more interesting. Using experimental techniques similar to those for 1D DMs, we have demonstrated 2D defect guiding as well. The experimental results are shown in Fig. 7.4. Here a 2D lattice with a single-site negative defect is first created in a 20 mm crystal as shown in Fig. 7.2. Then we launch a Gaussian probe beam into the defect (Fig. 7.4a). Under different lattice conditions, we observed different guided structures as shown in Fig. 7.4b–d. At lattice spacing of $27\ \mu\text{m}$ and bias field of 2.8 kV/cm, the Gaussian beam evolves into a DM, with most of its energy concentrated in the defect site (Fig. 7.4b). At spacing $42\ \mu\text{m}$ and bias field of 3.0 kV/cm, the tails along the principal axes of the square lattice (which are diagonally oriented) are more prominent, and they show interesting vortex-array-like structures (Fig. 7.4c). Figure 7.4d shows a typical interferogram corresponding to intensity pattern of Fig. 7.4c, where the locations of vortices are indicated by arrows. It is seen that the vortex cells have different sign of topological charge along two diagonal “tails” [45].

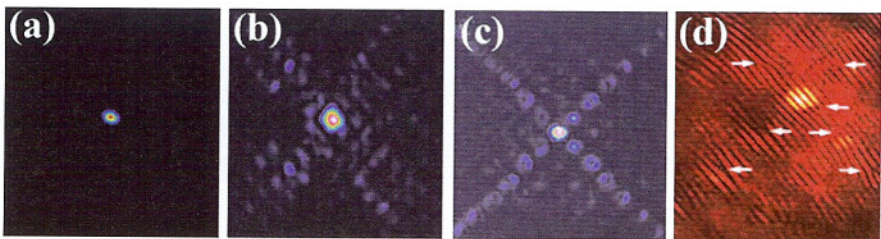


Fig. 7.4. Experimental observations on 2D defect guidance. (a) Input probe beam, (b), (c) intensity patterns of the output probe beam under different lattice conditions, (d) zoom-in interferogram of (c) with a tilted plane wave where arrows indicate location of vortices. The brightest spot corresponds to the defect site (after Ref. [45])